

The Nucleus of Comet 10P/Tempel 2 in 2013 and Consequences Regarding Its Rotational State: Early Science from the Discovery Channel Telescope

David G. Schleicher^{1,2}, Matthew M. Knight^{2,3}, Stephen E. Levine²

Submitted to *The Astronomical Journal* 2013 August 22; Accepted: 2013 September 10

ABSTRACT

We present new lightcurve measurements of Comet 10P/Tempel 2 carried out with Lowell Observatory's Discovery Channel Telescope in early 2013 when the comet was at aphelion. These data represent some of the first science obtained with this new 4.3-m facility. With Tempel 2 having been observed to exhibit a small but ongoing spin-down in its rotation period for over two decades, our primary goals at this time were two-fold. First, to determine its current rotation period and compare it to that measured shortly after its most recent perihelion passage in 2010, and second, to disentangle the spin-down from synodic effects due to the solar day and the Earth's orbital motion and to determine the sense of rotation, i.e. prograde or retrograde. At our midpoint of 2013 Feb 24, the observed synodic period is 8.948 ± 0.001 hr, exactly matching the predicted prograde rotation solution based on 2010 results, and yields a sidereal period of the identical value due to the solar and Earth synodic components just canceling out during the interval of the 2013 observations. The retrograde solution is ruled out because the associated sidereal periods in 2010 and 2013 are quite different even though we know that extremely little outgassing, needed to produce torques, occurred in this interval. With a definitive sense of rotation, the specific amounts of spin-down to the sidereal period could be assessed. The nominal values imply that the rate of spin-down has decreased over time, consistent with the secular drop in water production since 1988. Our data also exhibited an unexpectedly small lightcurve amplitude which appears to be associated with viewing from a large, negative sub-Earth latitude, and a lightcurve shape deviating from a simple sinusoid implying a highly irregularly shaped nucleus.

¹Contacting author: dgs@lowell.edu.

²Lowell Observatory, 1400 W. Mars Hill Rd, Flagstaff, AZ 86001, USA

³Visiting scientist at The Johns Hopkins University Applied Physics Laboratory, 11100 Johns Hopkins Road, Laurel, Maryland 20723, USA

Subject headings: comets: general — comets: individual (10P/Tempel 2) — methods: data analysis — methods: observational

1. INTRODUCTION

Comet 10P/Tempel 2 is the second largest Jupiter-family comet in existence – only 28P/Neujmin 1 is known to be larger – and is comparable in size to 1P/Halley. Unlike Halley, however, Tempel 2 has a very small fraction of its surface that is still active (<1%) and is therefore one of the most highly evolved comets. These two properties have made it possible to study its nucleus at both larger heliocentric distances (Jewitt & Meech 1988; Mueller & Ferrin 1996) and at favorable perihelion passages (Jewitt & Luu 1989; A’Hearn et al. 1989; Wisniewski 1990; Knight et al. 2011, 2012). It also exhibits a strong asymmetry about perihelion in brightness (Sekanina 1979) and production rates due to the seasonal effects associated with the orientation of the rotation axis and a small source region near one pole that dominates the outgassing (Knight et al. 2012). Of particular interest here is that Tempel 2 is one of the first comets to exhibit not just a change in its rotational period (Mueller & Ferrin 1996) but a progressive spin-down over multiple apparitions. Our lightcurve measurements obtained at the 1999 apparition gave a period of 8.941 ± 0.002 hr, about 32 s longer than the value of 8.932 ± 0.001 hr two orbits earlier in 1988 based on a reanalysis of all available data (Knight et al. 2011). We followed this with further measurements in 2010, finding a period of 8.950 ± 0.002 hr, thereby strongly implying the spin-down is caused by progressive torquing associated with the outgassing from the near-polar source region (Knight et al. 2012).

The situation, however, is somewhat more complicated than it first appears. While the measured spin-down was the same between 1988 and 1999, and between 1999 and 2010, the observations in the earlier apparitions were obtained several months prior to perihelion while the observations in 2010 were obtained between two and six months following perihelion. Thus a somewhat larger change in period was expected in the second pairing if the amount of torque remained the same at every perihelion passage. While our 2010 result might be explained by a secular decrease in outgassing that we observed during the past quarter century, it remained unclear what period Tempel 2 ultimately attained as it retreated from the Sun in 2011 and activity dropped off. Additionally, all of the reported values for its rotation period are synodic rather than sidereal. While some evidence has suggested that Tempel 2 is in prograde rotation (Sekanina 1991), a reanalysis of the same data gave conflicting results (Knight et al. 2011). Since the spin-down of the nucleus adds a further complication to extracting the sense of rotation from varying synodic effects, we considered the direction of rotation as being unresolved, resulting in a pair of possible side-

real periods for each synodic result. For example, the 2010 synodic value of 8.950 ± 0.002 hr corresponds to a prograde sidereal solution of 8.948 ± 0.002 hr or a retrograde solution of 8.955 ± 0.002 hr, where these offsets are asymmetric due to the Earth’s orbital motion. Since the difference between synodic and sidereal varies with orbital position and observer geometries, this results in an added ambiguity to the specific amount of torque delivered each apparition. Fortunately, the sense of rotation can be resolved with additional measurements of Tempel 2 at a more distant location in its orbit when the synodic/sidereal difference is much smaller than near perihelion.

With these motivations, and with access to our new 4-meter class Discovery Channel Telescope (DCT), we decided to again measure Tempel 2’s rotation period but this time near aphelion. The specific timing of the observations was based not only on the observing geometries but also required waiting for the comet to move sufficiently far away from the galactic plane. The initial night of planned observation also proved to be the first successful night of science operations for DCT, still early in its commissioning phase. We present here lightcurve data obtained over a 3-month interval, and the resulting derived period along with the implications of this result.

2. OBSERVATIONS AND REDUCTIONS

2.1. Instrumentation

Lowell Observatory’s Discovery Channel Telescope saw first light in April 2012, less than 7 years after ground-breaking. The telescope, with a 4.3-m primary, is located near Happy Jack, AZ, at an elevation of 2337 meters (cf. Levine et al. 2012; Bida et al. 2012). Site testing yielded a median seeing of 0.84 arcsec (Bida et al. 2004) and delivered images already routinely exhibit FWHM of ~ 0.8 arcsec when atmospheric conditions are good. The first instrument designed for DCT is the Large Monolithic Imager (LMI), which began service in September 2012. Containing a newly developed $6.1\text{K}\times 6.1\text{K}$ CCD by e2v, this camera yields a 12.3 arcmin on a side field-of-view at the $f/6.1$ Ritchey-Chretien focus (Massey et al. 2013). Our observations were obtained using 2×2 on-chip binning, resulting in a pixel scale of 0.240 arcsec, and we used a Kron-Cousins R band filter throughout.

2.2. Observations and Reductions

Successful and useful observations were acquired on two nights in January 2013, one in March, and two in April; planned observations in February were snowed out while limited

observations in May were interrupted by technical problems (including a regional power failure) making the remaining data useless for this project. Observational circumstances for each of the five useful nights are given in Table 1, including heliocentric distance (r_H), geocentric distance (Δ), and phase angle (θ). The January and March runs each immediately followed large storms, resulting in quite poor and variable seeing (~ 1.0 – 2.4 arcsec), while conditions were better in April (~ 0.9 – 1.3 arcsec); image quality additionally degraded at high airmasses as we attempted to maximize the temporal coverage each night. As expected during the very early science phase of a new telescope undergoing commissioning, a variety of small issues emerged and some affected the observations. In particular, pointing map problems in January required us to use the sidereal rate and manually guide on stars rather than track at Tempel 2’s rate of motion. Four-minute integrations were used, resulting in 1.6 arcsec of trailing of the comet. We were able to use our preferred mode of tracking at the comet’s rate of motion on the other runs, resulting in trailed comparison stars, though no tracking was actually required nor performed in April because the comet was within days of its stationary point. With a shorter exposure of 150 s and the slower rate of motion of the comet as it approached its stationary point, stellar trailing was quite small, 0.6 arcsec, in March while the comet trailed by <0.1 arcsec in April.

The choice of the aperture size for photometric extractions was, as usual, a compromise between a variety of factors, including trailing and seeing as just described, along with the contrast of the object to the sky, and how crowded the field was. The faintness of the comet and the occasional close passage of field stars argued for a small aperture while the other factors pushed for larger sizes, especially in January. Fortunately, as discussed below, no coma was detected and so no removal was necessary. We ultimately chose to minimize the resulting scatter in Tempel 2’s lightcurve each night, which resulted in aperture radii of 11 pixels (2.6 arcsec) in January, 8 pixels (1.9 arcsec) in March, and 6 pixels (1.4 arcsec) in April; sky measurements were obtained from the median value in an annulus between 30 and 60 pixels (7.2–14.4 arcsec). The effects of changing seeing were directly compensated for by using identical apertures for on-frame comparison stars (see below), while the differential effects associated with trailing were minimized with these relatively large extraction apertures.

Calibration was performed using standard techniques with the Interactive Data Language software package for removing bias and applying median twilight flat fields. An extinction coefficient of 0.098 mag per unit airmass was determined on Jan 13, and was applied to all of each nights’ data as a first-order correction for airmass. A minimum of seven comparison stars were used each night; the relatively slow motion of the comet at aphelion coupled with the large field of view of LMI meant these stars remained in the field throughout the night. Remaining variations from frame to frame due to cirrus, changing seeing, and second-order airmass effects were compensated for by determining and applying the median value

of the deviations of all the comparison stars. In practice, though the resulting standard deviations for the comparison stars were quite small, the scatter for the much fainter comet became unacceptable when this correction was larger than 0.5 mag, and we therefore excluded data above this threshold. We additionally excluded frames for which the comet was adversely affected by nearby stars, cosmic rays, etc. The uncertainties on each resulting measurement of Tempel 2 were based on the photometric uncertainties combined with the standard deviations of the comparison star corrections.

Absolute flux calibrations were applied by using SDSS r filter catalog values of each of our comparison stars. The average nightly uncertainty in the absolute flux calibrations was 0.06 mag, which encompasses both the uncertainty in the catalog magnitudes themselves and color effects in the extinction correction. The resulting nightly instrumental correction varied by as much as 0.3 mag because several nights had no interval when the sky was photometric. While Landolt fields were observed on the few photometric occasions, these measurements were too sparse to significantly improve the absolute calibration but did confirm that our calibration was good to better than 0.1 mag. Assuming a solar color, we applied an average offset of 0.22 mag to convert from SDSS r to Cousins R¹. Final lightcurve measurements and uncertainties of all 422 useful data points (as defined above) are listed in Table 2, as well as the observed mid-times for each image.

3. LIGHTCURVE RESULTS

3.1. Lightcurves

The reduced lightcurves are displayed in Figure 1 as a function of time for each of the five nights. Immediately evident is the large decrease in brightness during the apparition that will be shown later to be simply due to the combination of increasing distance and increasing phase angle. Gaps in the data on Jan 12 and the apparent late start on Jan 13 are due to clouds and/or the comet passing too close to a star. Series of images having the best effective seeing from Jan 13 and again from Apr 6 were stacked to search for evidence of a coma; none was detectable on either night. Comparison of the wings of the comet’s radial profile to stellar radial profiles on Apr 4 and Apr 6 (when the non-sidereal motion was negligible) suggests that any non-stellar component had an upper limit of 5% of the total cometary flux. Therefore no coma removal was required (or possible) from these observations, unlike observations near perihelion.

¹<http://www.sdss.org/dr5/algorithms/sdssUBVRITransform.html>

To remove the observed secular trend, we next performed a standard asteroidal normalization for these nuclear magnitudes to absolute values by correcting for heliocentric and geocentric distances and to zero phase angle, i.e. from the reduced magnitude, m_R , to $m_R(1,1,0)$. Our first attempts at normalization used the same linear phase function that we applied in our previous papers (Knight et al. 2011, 2012). This failed, however, to yield consistent brightnesses among the three observing runs no matter what phase coefficient was used. In retrospect, this was not surprising due to the much smaller phase angles involved in 2013 and the typical asteroidal non-linear opposition effect. Rather than empirically determining the needed curvature, we decided to use a model phase curve that best matched C-type asteroids, those with physical characteristics such as albedo most similar to comet nuclei. Fitting and interpolating the values from Table IV of Bowell & Lumme (1979), we computed phase adjustments (Δm_θ) for each night as given in Table 1. The resulting $m_R(1,1,0)$ values at lightcurve maxima were in remarkable agreement, indicating that the phase function for Tempel 2’s nucleus is indeed well-represented by C-type asteroids, and no further adjustments were applied.

3.2. Rotation Period

We continue to use our interactive period search routine for period determinations. As described in more detail in Knight et al. (2011), phase plots are instantaneously updated as we systematically step through possible periods and examine by eye the tightness of resulting lightcurves. Data are color-coded by date, making it easy to see small offsets in either brightness or phase throughout the phased curve. This is particularly useful when the intrinsic scatter due to photometric uncertainties is larger than usual, as we have here; a slightly incorrect period will only have a very slight increase in scatter and most period search algorithms will not “see” that one day is offset from another. In fact, we also used the phase dispersion minimization method (Stellingwerf 1978) and, while this gave the same result, its uncertainty is much greater than what can be easily estimated from the color-coded phase plots, i.e. when clear shifts between observing runs is evident. Note that standard routines can also misinterpret changes in the shape of the lightcurve, another factor here.

Our overall best observed period solution was 8.948 ± 0.001 hr, and the corresponding phase plot is shown in the top panel of Figure 2. Since there is no obvious preferred zero point for phasing, we choose 2013 Jan 0.0 as this placed zero phase away from interesting features and the ΔT values correspond to the day of the year; prior to phasing, the ΔT values were first corrected for light travel time from the observed mid-times in Table 1. As with previous apparitions, we have a double-peaked light curve where the two maxima are

nearly identical in brightness but the minima are quite different, with the deeper minimum nearly “V”-shaped while the smaller minimum varied in depth and shape with changing viewing geometry. Unfortunately, our phase coverage is incomplete in April and the shallower minimum is not sampled, so we cannot determine if the change in depth from January to March continued. Also evident is a ~ 0.02 mag shift of much (but not all) of the Jan 12 lightcurve from that of a day later on January 13, for which we have been unable to identify a cause. While this has no effect on the the period solution, it alters the perception of the shape for the first half of the lightcurve.

We also phased subsets of the data to look for evidence of a change in the observed period associated with the changing viewing geometries. As expected, phasing Jan/Apr yielded the same result as the entire data set, while a minor change was evident for the other two pairings – Jan/Mar gave a slightly smaller value (8.947 ± 0.001 hr) and Mar/Apr gave a slightly larger value (8.949 ± 0.002 hr) with the higher uncertainty in the latter value directly caused by the shorter interval. Within the uncertainties, this increase matches the predicted change of $+0.001$ hr, caused simply by the Earth’s orbital motion between our earliest midpoint pairing and the latest; the solar component to the synodic period near aphelion is both small and unchanging. These calculations all use the pole orientation from Knight et al. (2012) of R.A. = 162° and Dec. = $+58^\circ$ (and the diametrically opposite solution for retrograde rotation), but similar pole positions, such as from Sekanina (1991), would yield the same results.

As discussed in the Introduction, one goal of these observations was to uniquely discriminate between prograde and retrograde rotation for Tempel 2’s nucleus. The sense of rotation always determines the sign of the solar component of the synodic period while the Earth’s component is unaffected by the direction of rotation. At the midpoint of our ensemble of measurements for 2013, the solar and Earth components are coincidentally nearly identical and in the prograde case have opposite signs that cancel out, resulting in the sidereal period being the same as the synodic (8.948 ± 0.001 hr), while in the retrograde case they compound yielding a sidereal value of 8.950 ± 0.001 hr.

To determine which solution is correct, we next re-examine the solutions from 2010. Our overall observed (synodic) value was 8.950 ± 0.002 hr with a corresponding midpoint time of 2010 Oct 25 or 112 days following perihelion (Knight et al. 2012). Based on our water production rates throughout the apparition, over 95% of the total outgassing had taken place by this date. With an observed change in period of about $+0.004$ hr per perihelion passage, we concluded that further torquing late in the 2010 apparition should be negligible and that the sidereal period in 2013 would therefore be unchanged from the late 2010 result. The corresponding sidereal values at the 2010 midpoint are 8.948 hr (prograde) and 8.955 hr

(retrograde). Note that these values are slightly different from those listed in Knight et al. (2012) which erroneously only included the solar component but not the Earth’s component. With the expectation that the sidereal value should be the same in early 2013 as in late 2010, and the possible sidereal values in 2013 being 8.948 ± 0.001 hr (prograde) and 8.950 ± 0.001 hr (retrograde), we conclude that Tempel 2 *must* be in prograde rotation, with a sidereal period in late 2010 and in early 2013 of 8.948 hr.

As further evidence that Tempel 2 is in a prograde rotation, we also examined the retrograde scenario. If it was the retrograde case, then as already stated the sidereal period in 2010 would have been 8.955 hr. Since the difference between the retrograde synodic and sidereal periods in 2013 would be -0.002 hr, we should have measured a period of 8.953 hr. Phasing with this value is shown in the bottom panel of Figure 2 and it is clear that this solution does not yield a viable lightcurve, therefore the comet must instead be in prograde rotation.

Looking back at the earlier apparitions requires disentangling the synodic effects from the actual changes in period due to torquing. An early attempt to derive the sidereal period from the changing synodic period during 1988 (Sekanina 1991) suffered from several problems, including the claim of a smoothly decreasing period which could not be reproduced during a detailed reanalysis (Knight et al. 2011) and our new determination that his synodic/sidereal modeling only included the Earth’s motion but neglected the dominant solar component. Having now definitively determined the sense of rotation as prograde, we can reexamine prior apparitions. The computed sidereal periods for each epoch are given in Table 3; for completeness and to illustrate the asymmetries of the pro- and retrograde solutions with respect to the observed synodic periods, we also tabulate the retrograde values. Again, these values differ somewhat from the values given in Knight et al. (2012) since the Earth component is now included along with the solar component, thereby causing the asymmetry. Our conclusions regarding a decrease in the amount of spin-down remain unchanged from Knight et al. (2012), with sidereal periods before perihelia in 1988 of 8.931 hr and in 1999 of 8.939 hr, for an average spin-down by 0.004 hr per apparition. The same rate of spin-down would have predicted a sidereal period of 8.951 hr in late 2010, a larger change than we observe. We continue to think the most likely cause of this is the decrease in total water production from 1988 to 1999 and to 2010, with lower production rates providing a smaller amount of torquing. However, within the uncertainties of the period determinations, the data are also consistent with no change in the rate of spin-down. The agreement between the late 1994 period with early 1999 also remains, with both yielding a sidereal period of 8.939 hr during an interval for which there was not an intervening perihelion passage.

3.3. Nucleus Cross-Section

Our 2013 lightcurves of Tempel 2 revealed two unexpected findings. First, the amplitude within the lightcurve was smaller than we had assumed it would be and, second, the peak brightness was higher than predicted from earlier apparitions even after compensating for a non-linear phase function. After considering a variety of possibilities, such as removing too much or too little coma for differing apparitions or systematic effects when different filters were used, we think we have arrived at a self-consistent explanation. Our expectations for 2013 were based on assuming that Tempel 2 is a prolate ellipsoid with similar dimensions for the small and intermediate axes while the long axis is about $2.1\times$ greater. This is based on the 1988 thermal IR lightcurve from A’Hearn et al. (1989) and that the sub-Earth latitude then varied between -1° and -9° , i.e. the comet was viewed in 1988 nearly equator-on using our preferred pole solution. In early 2013, the sub-Earth latitude was -47° , yielding a predicted amplitude of 0.4 mag, significantly greater than the observed value of ~ 0.2 mag. If, however, the intermediate axis is actually intermediate in length rather than the same as the small axis, then the total cross-section will appear to increase as one views from more pole-on and the amplitude will become even smaller than the simple function of the cosine of the sub-Earth latitude (the intermediate axis begins to dominate over the small axis). Note that in this tri-axial case, it is the ratio of the long axis to the intermediate axis that determines the amplitude for the equator-on view. Therefore, to explain the 1988 amplitude, the intermediate axis remains the same as originally assumed for the prolate case, and it is the short axis which must be even shorter. For our observed amplitude in 2013, this requires the short axis to be less than one-third that of long axis, while the intermediate axis remains at about one-half of the long axis. This implies an even more elongated nucleus than the tri-axial solution with ratios of 0.43 : 0.60 : 1.0 proposed by Sekanina (1991). In addition to explaining the observed amplitude, our tri-axial solution also naturally explains the increased brightness at lightcurve maxima in 2013 as being due to the increased total cross-section relative to the equator-on view.

We strongly suspect, however, that the shape of the nucleus significantly departs from a tri-axial ellipsoid for several reasons. The lightcurve shape is not sinusoidal, but rather has one "V"-shaped minimum and one rounded minimum. Also, the shapes and depths of the minima change rapidly in 2013 with only a small change in viewing geometries even though the sub-Earth and sub-solar latitudes did not vary. Finally, as discussed below, the amplitudes are quite different when the comet was viewed from high positive latitudes as compared to high negative latitudes. Thus, we conclude that the nucleus must have large-scale protuberances.

To first-order, the tri-axial ellipsoid explains most of the brightness and amplitudes

measured at the other apparitions. Most similar to 2013 were the circumstance in early 1987 with a sub-Earth latitude of -52° , and where Jewitt & Meech (1988) measured an amplitude of ~ 0.3 mag and a peak magnitude essentially identical to our 2013 value once adjustments are made for filter and phase angle. The 1999 apparition was nearly identical to that of 1988, and the lightcurve characteristics are also essentially the same. The peak brightness in 1994 (Mueller & Ferrin 1996) is also consistent with 1988 and 1999 but the amplitude is somewhat smaller (by ~ 0.1 – 0.2 mag) with no clear explanation since the sub-Earth latitude was close to the equator. Most different were our results from 2010 (Knight et al. 2012), where the peak brightness is ~ 0.2 – 0.3 mag fainter while the amplitude is larger than expected for a sub-Earth latitude near $+40^\circ$. While an over removal of coma might partially explain both aspects, our methodology was the same used for the 1999 apparition which has no such issues, leading us to suspect that Tempel 2’s actual shape characteristics are another significant factor; this is supported by the fact that only in 2010 did the sub-Earth latitude have a high positive value ($+40^\circ$) while all other apparitions were either near the equator (1988, 1994, 1999) or at high negative values (1987, 2013).

4. DISCUSSION AND SUMMARY

The observations reported here represent some of the first science collected with Lowell Observatory’s new Discovery Channel Telescope. Despite a few problems associated with a facility still in the early stages of commissioning, we were able to easily fulfill our major science objectives regarding Comet Tempel 2’s rotational state, in spite of a smaller lightcurve amplitude than expected. We obtained a precise measurement of its current rotation period that, when combined with our 2010 measurements, yielded a definitive determination of its sense of rotation. This result in turn allowed us to determine the correct sidereal period associated with observed synodic values at each prior apparition. For Lowell Observatory and its partners, a new era has begun in which projects requiring time-intensive or long-duration observations can be accomplished for targets much fainter than have ever been possible. In the specific case of comet nuclei, we can now measure lightcurves of comet nuclei far from perihelion.

The measured periodicity in a nucleus lightcurve depends on the changing cross-section both as illuminated by the Sun and as seen from the Earth, and in turn depends on the solar day as well as the Earth’s motion with respect to the comet and the Sun. Disentangling these effects from the change in the physical rotation due to torquing had been problematic at best. However, the relative importance of the solar component and Earth’s motion component are quite different far from the Sun as compared to near perihelion. Because of this, we

planned and executed these new observations. The resulting synodic period, 8.948 ± 0.001 hr, matched that expected for the prograde scenario from 2010 while the nominal period associated with the retrograde solution is clearly ruled out. We therefore conclude that Tempel 2’s rotation is prograde with respect to both the ecliptic and to its orbital plane. The sidereal period, 8.948 ± 0.001 hr, is coincidentally identical to the synodic value as the solar and Earth components of the synodic period just cancel out during the interval of our 2013 observations. The new data also confirm that no additional spin-down took place following our late 2010 measurements, consistent with the water production curve showing a near-cessation of activity by that time. This lack of a change in the sidereal period very late in the 2010 apparition thereby implies that the smaller change in the period per perihelion passage between 1999 and 2010 as compared to 1988 to 1999 is real (although a constant rate of spin-down cannot be excluded within the uncertainties). Note that the inferred changes match those given by Knight et al. (2012) for the prograde case. Thus our hypothesis that a decrease in torquing is associated with the secular decrease in water production from 1988 to 2010 is probably correct. We note, however, that there is no strong evidence for a long-term decrease in activity over the past century, and the secular drop over the past two decades may reverse as the surface is eroded and varying proportions of ice are exposed from successive perihelion passages.

Similar to prior apparitions, the light curve is double-peaked with near-equal maxima but quite differently shaped minima. The shape and depth of one of the minima also changed over the three-month interval, another trait observed in the past. Both characteristics directly indicate that the shape of Tempel 2’s nucleus is not a simple prolate ellipsoid or even a triaxial ellipsoid but must instead have large-scale protuberances to cause such clear changes in the lightcurve from such a small change in viewing geometries ($< 20^\circ$) and essentially no change in sub-Earth and sub-solar latitudes. The unexpectedly small amplitude we measured in the lightcurve (~ 0.2 mag) appears to also be due to peculiarities of the nucleus shape – our value is in good agreement with the only other data obtained at a similar sub-Earth latitude (Jewitt & Meech 1988), while data taken from near-equator on or from the other hemisphere all exhibit a much larger amplitude. The data further suggest that the length of the short axis is substantially shorter than that of the intermediate axis, though the shape is probably not as extreme as that of Comet 103P/Hartley 2 as imaged from EPOXI (A’Hearn et al. 2011). Thus a more complete story of the properties of Tempel 2’s nucleus is beginning to emerge. While determining the detailed shape must continue to await an upclose view – Tempel 2 was the proposed target of the planned Comet Rendezvous Asteroid Flyby mission more than two decades ago – additional numerical modeling and new investigations from afar can continue to reveal clues to its physical structure and evolving behavior.

ACKNOWLEDGMENTS

We thank T. Farnham for calculations of the offsets between the prograde and retrograde synodic periods with respect to a given sidereal period. We gratefully acknowledge the assistance of M. Fendrock with the first observing run and preliminary analyses, and A. Venetiou, M. Sweaton, J. Sanborn, R. Winner, and S. Strosahl for their successful operations during the early commissioning phase of the DCT, thereby making these observations possible. We also thank R. Millis, W. L. Putnam, and J. Hendricks for their vision and support which allowed the DCT to become a reality, and all members of the DCT and LMI teams.

These results made use of Lowell Observatory’s Discovery Channel Telescope, supported by Lowell, Discovery Communications, Boston University, the University of Maryland, and the University of Toledo. M.M.K. is grateful for office space provided by the University of Maryland Department of Astronomy and Johns Hopkins University Applied Physics Laboratory while working on this project. The LMI instrument was funded by the National Science Foundation via grant AST-1005313. This research has been supported by NASA’s Planetary Astronomy Program (Grant NNX09AB51G).

REFERENCES

- A’Hearn, M. F., Campins, H., Schleicher, D. G., & Millis, R. L. 1989, *ApJ*, 347, 1155
- A’Hearn, M. F., Belton, M. J. S., Delamere, W. A., et al. 2011, *Science*, 332, 1396
- Bida, T. A., Dunham, E. W., Bright, L. P., & Corson, C. 2004, in *Ground-based Telescopes*. Ed. J. M. Oschmann, Jr., *Proc. of SPIE*, 5489, 196
- Bida, T. A., Dunham, E. W., Nye, R. A., Chylek, T., & Oliver, R. C. 2012, in *Ground-based and Airborne Telescopes IV.*, Eds. L. M. Stepp, R. Gilmozzi, H. J. Hall, *Proc. of SPIE*, 8444, 844451
- Bowell, E., & Lumme, K. 1979, *Colorimetry and magnitudes of asteroids*, Ed. T. Gehrels, 132–169
- Jewitt, D., & Luu, J. 1989, *AJ*, 97, 1766
- Jewitt, D. C., & Meech, K. J. 1988, *ApJ*, 328, 974
- Knight, M. M., Farnham, T. L., Schleicher, D. G., & Schwieterman, E. W. 2011, *AJ*, 141, 2
- Knight, M. M., Schleicher, D. G., Farnham, T. L., Schwieterman, E. W., & Christensen, S. R. 2012, *AJ*, 144, 153

Levine, S. E., Bida, T. A., Chylek, T., et al. 2012, in Ground-based and Airborne Telescopes IV., Eds. L. M. Stepp, R. Gilmozzi, H. J. Hall, Proc. of SPIE, 8444, 844419

Massey, P., Dunham, E. W., Bida, T. A., et al. 2013, AAS Meeting #221, poster #345.02

Mueller, B. E. A., & Ferrin, I. 1996, Icarus, 123, 463

Sekanina, Z. 1979, Icarus, 37, 420

—. 1991, AJ, 102, 350

Stellingwerf, R. F. 1978, ApJ, 224, 953

Wisniewski, W. Z. 1990, Icarus, 86, 52

This preprint was prepared with the AAS L^AT_EX macros v5.2.

Table 1. Summary of Tempel 2 observational circumstances in 2013. ^a

UT Date	UT	ΔT^b (day)	r_H (AU)	Δ (AU)	θ ($^\circ$)	Δm_θ^c (mag)	Ecl. Long. Earth ($^\circ$) ^d	Ecl. Long. Sun ($^\circ$) ^e	Conditions
Jan 12	3:34–13:29	+12.4	4.697	3.770	4.5	0.42	203.8	309.3	Clouds
Jan 13	3:35–13:27	+13.4	4.698	3.765	4.3	0.41	204.1	309.4	Intermittent clouds
Mar 11	2:51–10:38	+70.3	4.709	3.970	8.8	0.64	225.4	313.1	Cirrus
Apr 4	3:01– 8:52	+94.2	4.707	4.293	11.6	0.76	234.6	314.6	Cirrus
Apr 6	2:56– 8:45	+96.2	4.706	4.323	11.8	0.76	235.5	314.8	Clouds

^aAll parameters were taken at the midpoint of each night’s observations.

^bTime since 2013 Jan 0.0.

^cMagnitude correction to normalize to $\theta = 0^\circ$.

^dEcliptic longitude of the Earth as seen from the comet.

^eEcliptic longitude of the Sun as seen from the comet.

Table 2. Photometry of Comet Tempel 2 in 2013

Date ^a	UT ^b	m _R ^c	σ_{m_R} ^d	Date ^a	UT ^b	m _R ^c	σ_{m_R} ^d	Date ^a	UT ^b	m _R ^c	σ_{m_R} ^d	Date ^a	UT ^b	m _R ^c	σ_{m_R} ^d
Jan 12	4.188	20.025	0.039	Jan 13	7.857	20.109	0.013	Mar 11	2.983	20.433	0.022	Mar 11	7.064	20.482	0.023
Jan 12	6.337	20.216	0.031	Jan 13	7.931	20.110	0.013	Mar 11	3.040	20.456	0.023	Mar 11	7.112	20.458	0.023
Jan 12	6.486	20.209	0.027	Jan 13	8.005	20.126	0.012	Mar 11	3.090	20.434	0.021	Mar 11	7.161	20.465	0.022
Jan 12	6.635	20.230	0.027	Jan 13	8.079	20.136	0.013	Mar 11	3.199	20.436	0.022	Mar 11	7.209	20.446	0.021
Jan 12	6.710	20.224	0.023	Jan 13	8.153	20.114	0.013	Mar 11	3.250	20.434	0.020	Mar 11	7.258	20.455	0.021
Jan 12	6.786	20.247	0.026	Jan 13	8.226	20.119	0.013	Mar 11	3.300	20.392	0.020	Mar 11	7.307	20.444	0.022
Jan 12	6.861	20.208	0.030	Jan 13	8.301	20.144	0.013	Mar 11	3.350	20.386	0.020	Mar 11	7.355	20.449	0.023
Jan 12	6.936	20.237	0.029	Jan 13	8.374	20.152	0.012	Mar 11	3.413	20.407	0.021	Mar 11	7.403	20.478	0.025
Jan 12	7.011	20.259	0.032	Jan 13	8.448	20.177	0.013	Mar 11	3.464	20.387	0.020	Mar 11	7.451	20.455	0.023
Jan 12	9.159	20.054	0.016	Jan 13	8.522	20.170	0.013	Mar 11	3.514	20.398	0.021	Mar 11	7.503	20.446	0.021
Jan 12	9.235	20.112	0.015	Jan 13	8.597	20.173	0.013	Mar 11	3.576	20.396	0.022	Mar 11	7.552	20.459	0.021
Jan 12	9.309	20.077	0.014	Jan 13	8.676	20.166	0.012	Mar 11	3.630	20.403	0.023	Mar 11	7.600	20.431	0.020
Jan 12	9.384	20.079	0.014	Jan 13	8.750	20.180	0.012	Mar 11	3.681	20.389	0.023	Mar 11	7.648	20.417	0.019
Jan 12	9.458	20.064	0.013	Jan 13	8.824	20.169	0.013	Mar 11	3.736	20.393	0.022	Mar 11	7.696	20.421	0.020
Jan 12	9.533	20.034	0.013	Jan 13	8.898	20.182	0.013	Mar 11	3.793	20.395	0.022	Mar 11	7.746	20.429	0.022
Jan 12	9.607	20.030	0.013	Jan 13	9.195	20.213	0.013	Mar 11	3.846	20.413	0.023	Mar 11	7.795	20.435	0.022
Jan 12	9.681	20.067	0.013	Jan 13	9.268	20.220	0.013	Mar 11	3.895	20.394	0.022	Mar 11	7.843	20.406	0.022
Jan 12	9.756	20.076	0.014	Jan 13	9.342	20.224	0.014	Mar 11	3.945	20.411	0.022	Mar 11	7.891	20.461	0.023
Jan 12	9.830	20.075	0.013	Jan 13	9.416	20.213	0.013	Mar 11	3.994	20.396	0.020	Mar 11	7.939	20.445	0.023
Jan 12	9.905	20.089	0.015	Jan 13	9.490	20.216	0.013	Mar 11	4.045	20.387	0.021	Mar 11	7.990	20.418	0.022
Jan 12	9.979	20.107	0.015	Jan 13	9.564	20.235	0.013	Mar 11	4.098	20.390	0.021	Mar 11	8.039	20.443	0.021
Jan 12	10.055	20.116	0.014	Jan 13	9.638	20.193	0.013	Mar 11	4.147	20.415	0.022	Mar 11	8.087	20.395	0.022
Jan 12	10.130	20.116	0.016	Jan 13	9.934	20.176	0.013	Mar 11	4.196	20.424	0.021	Mar 11	8.135	20.431	0.020
Jan 12	10.428	20.114	0.022	Jan 13	10.008	20.181	0.012	Mar 11	4.244	20.423	0.022	Mar 11	8.184	20.418	0.020
Jan 12	10.576	20.136	0.023	Jan 13	10.082	20.167	0.013	Mar 11	4.294	20.451	0.022	Mar 11	8.237	20.430	0.021
Jan 12	10.651	20.132	0.016	Jan 13	10.156	20.172	0.012	Mar 11	4.751	20.434	0.024	Mar 11	8.285	20.391	0.021
Jan 12	10.725	20.128	0.017	Jan 13	10.230	20.126	0.012	Mar 11	4.801	20.451	0.025	Mar 11	8.334	20.443	0.022
Jan 12	10.800	20.139	0.016	Jan 13	10.304	20.132	0.012	Mar 11	4.852	20.473	0.025	Mar 11	8.382	20.400	0.022
Jan 12	10.873	20.110	0.017	Jan 13	10.380	20.133	0.012	Mar 11	4.907	20.478	0.027	Mar 11	8.430	20.422	0.024
Jan 12	10.948	20.106	0.016	Jan 13	10.454	20.136	0.012	Mar 11	4.956	20.494	0.027	Mar 11	8.496	20.394	0.023
Jan 12	11.022	20.136	0.015	Jan 13	10.528	20.150	0.012	Mar 11	5.005	20.504	0.026	Mar 11	8.545	20.407	0.023
Jan 12	11.096	20.159	0.015	Jan 13	10.601	20.119	0.012	Mar 11	5.054	20.491	0.027	Mar 11	8.593	20.440	0.024
Jan 12	11.170	20.131	0.014	Jan 13	10.675	20.104	0.012	Mar 11	5.102	20.511	0.027	Mar 11	8.641	20.419	0.024
Jan 12	11.245	20.114	0.014	Jan 13	10.750	20.103	0.012	Mar 11	5.151	20.485	0.025	Mar 11	8.689	20.464	0.025
Jan 12	11.319	20.106	0.014	Jan 13	10.824	20.088	0.012	Mar 11	5.199	20.504	0.025	Mar 11	8.737	20.473	0.026
Jan 12	11.394	20.158	0.015	Jan 13	10.898	20.067	0.012	Mar 11	5.248	20.535	0.024	Mar 11	8.886	20.468	0.026
Jan 12	11.544	20.145	0.023	Jan 13	10.972	20.070	0.012	Mar 11	5.296	20.509	0.025	Mar 11	8.935	20.472	0.027
Jan 12	11.916	20.149	0.023	Jan 13	11.046	20.081	0.012	Mar 11	5.345	20.565	0.030	Mar 11	8.983	20.488	0.027
Jan 12	12.065	20.111	0.023	Jan 13	11.121	20.063	0.012	Mar 11	5.393	20.543	0.027	Mar 11	9.031	20.455	0.028
Jan 12	12.215	20.077	0.016	Jan 13	11.417	20.056	0.012	Mar 11	5.441	20.526	0.028	Mar 11	9.079	20.499	0.030
Jan 12	12.363	20.119	0.014	Jan 13	11.490	20.038	0.012	Mar 11	5.515	20.539	0.029	Mar 11	9.129	20.447	0.032
Jan 12	12.688	20.045	0.016	Jan 13	11.565	20.048	0.012	Mar 11	5.564	20.526	0.028	Mar 11	9.178	20.494	0.032
Jan 13	5.839	20.120	0.019	Jan 13	11.640	20.059	0.012	Mar 11	5.612	20.508	0.023	Mar 11	9.226	20.458	0.029
Jan 13	5.987	20.140	0.015	Jan 13	11.713	20.051	0.012	Mar 11	5.660	20.527	0.025	Mar 11	9.274	20.501	0.031
Jan 13	6.061	20.139	0.014	Jan 13	11.787	20.043	0.012	Mar 11	5.708	20.520	0.025	Mar 11	9.323	20.462	0.032
Jan 13	6.136	20.150	0.014	Jan 13	11.861	20.057	0.012	Mar 11	5.758	20.496	0.022	Mar 11	9.373	20.494	0.034
Jan 13	6.211	20.125	0.014	Jan 13	11.935	20.043	0.012	Mar 11	5.806	20.497	0.024	Mar 11	9.421	20.504	0.037
Jan 13	6.285	20.119	0.014	Jan 13	12.009	20.062	0.013	Mar 11	5.951	20.476	0.024	Mar 11	9.469	20.536	0.038
Jan 13	6.359	20.097	0.013	Jan 13	12.083	20.063	0.013	Mar 11	6.002	20.541	0.024	Mar 11	9.518	20.499	0.036
Jan 13	6.433	20.105	0.013	Jan 13	12.157	20.051	0.013	Mar 11	6.050	20.542	0.024	Mar 11	9.566	20.537	0.038
Jan 13	6.509	20.097	0.013	Jan 13	12.231	20.060	0.013	Mar 11	6.099	20.529	0.025	Mar 11	9.616	20.492	0.037
Jan 13	6.583	20.100	0.013	Jan 13	12.305	20.071	0.013	Mar 11	6.147	20.515	0.025	Mar 11	9.664	20.489	0.043
Jan 13	6.658	20.102	0.013	Jan 13	12.379	20.097	0.014	Mar 11	6.195	20.530	0.027	Mar 11	9.712	20.532	0.040
Jan 13	6.731	20.112	0.013	Jan 13	12.454	20.093	0.014	Mar 11	6.243	20.499	0.024	Mar 11	9.760	20.596	0.042
Jan 13	6.805	20.099	0.013	Jan 13	12.528	20.099	0.014	Mar 11	6.292	20.552	0.024	Mar 11	9.809	20.567	0.041
Jan 13	6.879	20.089	0.013	Jan 13	12.602	20.096	0.015	Mar 11	6.340	20.545	0.025	Mar 11	9.866	20.607	0.042
Jan 13	6.953	20.074	0.013	Jan 13	12.676	20.080	0.015	Mar 11	6.388	20.475	0.024	Mar 11	9.915	20.579	0.039
Jan 13	7.027	20.099	0.013	Jan 13	12.750	20.106	0.015	Mar 11	6.437	20.503	0.023	Mar 11	9.963	20.599	0.041
Jan 13	7.101	20.123	0.013	Jan 13	12.899	20.111	0.016	Mar 11	6.675	20.486	0.038	Mar 11	10.011	20.533	0.040
Jan 13	7.176	20.072	0.013	Jan 13	12.973	20.119	0.018	Mar 11	6.722	20.506	0.025	Mar 11	10.059	20.609	0.044
Jan 13	7.250	20.085	0.013	Jan 13	13.047	20.111	0.016	Mar 11	6.773	20.473	0.023	Mar 11	10.109	20.537	0.046
Jan 13	7.323	20.067	0.012	Jan 13	13.121	20.115	0.017	Mar 11	6.821	20.462	0.023	Mar 11	10.157	20.592	0.048
Jan 13	7.398	20.055	0.012	Jan 13	13.195	20.130	0.020	Mar 11	6.869	20.478	0.024	Mar 11	10.206	20.582	0.049
Jan 13	7.472	20.071	0.013	Jan 13	13.269	20.159	0.020	Mar 11	6.917	20.479	0.022	Mar 11	10.254	20.610	0.053
Jan 13	7.546	20.098	0.013	Jan 13	13.344	20.142	0.020	Mar 11	6.966	20.460	0.023	Mar 11	10.302	20.561	0.051
Jan 13	7.620	20.102	0.012	Mar 11	2.850	20.446	0.033	Mar 11	7.016	20.475	0.024	Mar 11	10.354	20.610	0.054

Table 2—Continued

Date ^a	UT ^b	m _R ^c	σ _{m_R} ^d	Date ^a	UT ^b	m _R ^c	σ _{m_R} ^d	Date ^a	UT ^b	m _R ^c	σ _{m_R} ^d	Date ^a	UT ^b	m _R ^c	σ _{m_R} ^d
Apr 4	3.028	20.766	0.044	Apr 4	4.973	20.710	0.025	Apr 4	7.177	20.829	0.031	Apr 6	4.040	20.890	0.028
Apr 4	3.071	20.767	0.027	Apr 4	5.021	20.732	0.026	Apr 4	7.225	20.853	0.031	Apr 6	4.090	20.926	0.033
Apr 4	3.127	20.775	0.028	Apr 4	5.069	20.691	0.026	Apr 4	7.275	20.795	0.031	Apr 6	4.138	20.889	0.027
Apr 4	3.176	20.773	0.028	Apr 4	5.117	20.657	0.025	Apr 4	7.323	20.842	0.032	Apr 6	4.186	20.859	0.026
Apr 4	3.224	20.794	0.028	Apr 4	5.166	20.711	0.029	Apr 4	7.371	20.794	0.033	Apr 6	4.235	20.910	0.026
Apr 4	3.275	20.723	0.028	Apr 4	5.220	20.719	0.028	Apr 4	7.419	20.844	0.033	Apr 6	4.283	20.917	0.026
Apr 4	3.323	20.706	0.025	Apr 4	5.268	20.727	0.027	Apr 4	7.468	20.833	0.033	Apr 6	4.333	20.893	0.025
Apr 4	3.371	20.738	0.027	Apr 4	5.316	20.708	0.027	Apr 4	7.522	20.802	0.034	Apr 6	4.381	20.855	0.024
Apr 4	3.420	20.776	0.028	Apr 4	5.364	20.713	0.027	Apr 4	7.570	20.830	0.036	Apr 6	4.429	20.858	0.024
Apr 4	3.468	20.758	0.029	Apr 4	5.412	20.689	0.026	Apr 4	7.618	20.820	0.037	Apr 6	4.478	20.857	0.024
Apr 4	3.517	20.722	0.028	Apr 4	5.468	20.735	0.027	Apr 4	7.666	20.745	0.037	Apr 6	4.526	20.862	0.025
Apr 4	3.566	20.772	0.027	Apr 4	5.716	20.731	0.026	Apr 4	7.715	20.824	0.042	Apr 6	4.575	20.854	0.025
Apr 4	3.614	20.724	0.025	Apr 4	5.781	20.739	0.026	Apr 4	7.764	20.766	0.042	Apr 6	4.624	20.826	0.025
Apr 4	3.662	20.764	0.027	Apr 4	5.829	20.732	0.026	Apr 4	7.812	20.797	0.037	Apr 6	4.672	20.821	0.027
Apr 4	3.711	20.759	0.026	Apr 4	5.878	20.760	0.026	Apr 4	7.860	20.804	0.036	Apr 6	4.855	20.829	0.033
Apr 4	3.760	20.769	0.026	Apr 4	5.926	20.782	0.026	Apr 4	7.908	20.835	0.038	Apr 6	4.952	20.811	0.030
Apr 4	3.808	20.735	0.026	Apr 4	5.974	20.769	0.026	Apr 4	7.957	20.814	0.038	Apr 6	5.243	20.747	0.028
Apr 4	3.857	20.750	0.025	Apr 4	6.023	20.758	0.027	Apr 4	8.006	20.855	0.037	Apr 6	5.291	20.763	0.028
Apr 4	3.905	20.728	0.026	Apr 4	6.072	20.784	0.026	Apr 4	8.054	20.839	0.038	Apr 6	5.341	20.740	0.027
Apr 4	3.953	20.784	0.027	Apr 4	6.120	20.790	0.027	Apr 4	8.102	20.773	0.034	Apr 6	5.389	20.794	0.029
Apr 4	4.002	20.714	0.028	Apr 4	6.168	20.764	0.026	Apr 4	8.151	20.781	0.035	Apr 6	5.437	20.745	0.036
Apr 4	4.051	20.756	0.028	Apr 4	6.216	20.786	0.026	Apr 4	8.199	20.797	0.037	Apr 6	5.486	20.743	0.031
Apr 4	4.099	20.758	0.026	Apr 4	6.305	20.790	0.026	Apr 4	8.250	20.737	0.036	Apr 6	5.534	20.743	0.025
Apr 4	4.147	20.710	0.025	Apr 4	6.354	20.805	0.027	Apr 4	8.298	20.763	0.038	Apr 6	5.583	20.735	0.025
Apr 4	4.195	20.724	0.026	Apr 4	6.402	20.795	0.028	Apr 4	8.346	20.741	0.038	Apr 6	5.631	20.696	0.024
Apr 4	4.244	20.744	0.028	Apr 4	6.450	20.819	0.028	Apr 4	8.394	20.750	0.053	Apr 6	5.679	20.741	0.025
Apr 4	4.292	20.710	0.025	Apr 4	6.498	20.817	0.028	Apr 4	8.442	20.754	0.045	Apr 6	5.728	20.731	0.025
Apr 4	4.341	20.719	0.024	Apr 4	6.547	20.823	0.029	Apr 4	8.498	20.798	0.051	Apr 6	5.776	20.716	0.025
Apr 4	4.389	20.716	0.024	Apr 4	6.595	20.850	0.030	Apr 4	8.546	20.756	0.048	Apr 6	5.825	20.707	0.025
Apr 4	4.438	20.684	0.026	Apr 4	6.644	20.851	0.029	Apr 4	8.594	20.751	0.049	Apr 6	5.873	20.705	0.024
Apr 4	4.488	20.698	0.023	Apr 4	6.692	20.835	0.029	Apr 4	8.642	20.699	0.050	Apr 6	5.921	20.719	0.025
Apr 4	4.536	20.687	0.023	Apr 4	6.740	20.810	0.030	Apr 4	8.740	20.729	0.055	Apr 6	5.970	20.704	0.026
Apr 4	4.584	20.712	0.023	Apr 4	6.790	20.855	0.031	Apr 6	3.029	20.856	0.134	Apr 6	6.018	20.728	0.027
Apr 4	4.632	20.724	0.023	Apr 4	6.839	20.817	0.031	Apr 6	3.646	20.858	0.027	Apr 6	6.067	20.724	0.027
Apr 4	4.680	20.719	0.023	Apr 4	6.887	20.850	0.032	Apr 6	3.701	20.865	0.027	Apr 6	6.115	20.727	0.027
Apr 4	4.730	20.727	0.024	Apr 4	6.935	20.894	0.033	Apr 6	3.749	20.920	0.027	Apr 6	6.164	20.725	0.027
Apr 4	4.779	20.699	0.025	Apr 4	6.983	20.877	0.031	Apr 6	3.797	20.875	0.027	Apr 6	6.212	20.715	0.029
Apr 4	4.827	20.672	0.026	Apr 4	7.032	20.824	0.029	Apr 6	3.847	20.888	0.025	Apr 6	6.260	20.710	0.028
Apr 4	4.875	20.684	0.025	Apr 4	7.080	20.867	0.030	Apr 6	3.895	20.901	0.027				
Apr 4	4.923	20.711	0.025	Apr 4	7.129	20.859	0.031	Apr 6	3.992	20.901	0.028				

^aUT date of observations.

^bUT at midpoint of the exposure (uncorrected for light travel time).

^cObserved R-band magnitude (after applying absolute calibrations, extinction corrections, and comparison star corrections).

^dUncertainty in the observed magnitude.

Table 3. Sidereal Rotation Periods and Lightcurve Amplitudes

UT date ^a	Synodic	Sidereal Period (hr) ^b		Amplitude (mag)	Sub-Earth Latitude (°)	Sub-Solar Latitude (°)
	Period (hr)	Prograde ^c	Retrograde			
1987 Apr 1	—	—	—	0.3	–52	–46
1988 Apr 28	8.932 ± 0.001	8.931	8.935	0.5 – 0.8	–2 – –10	–18 – +17
1994 Nov 22	8.939 ± 0.003	8.939	8.941	0.5	–3 – +4	+2 – –7
1999 May 20	8.941 ± 0.002	8.939	8.945	0.5 – 0.7	+9 – +10	–1 – +21
2010 Oct 25	8.950 ± 0.002	8.948	8.955	0.5 – 0.8	+35 – +43	+40 – +13
2013 Feb 24	8.948 ± 0.001	8.948	8.950	0.2	–47	–48

^aMidpoint of the observations used to determine the synodic period. The relevant perihelion dates are 1988 Sep 16, 1994 Mar 16, 1999 Sep 8, 2005 Feb 15, 2010 Jul 4, and 2015 Nov 14.

^bThe estimated uncertainties are identical to those listed in column 2.

^cThe combined 2010 and 2013 results reveal that Tempel 2 is in prograde rotation.

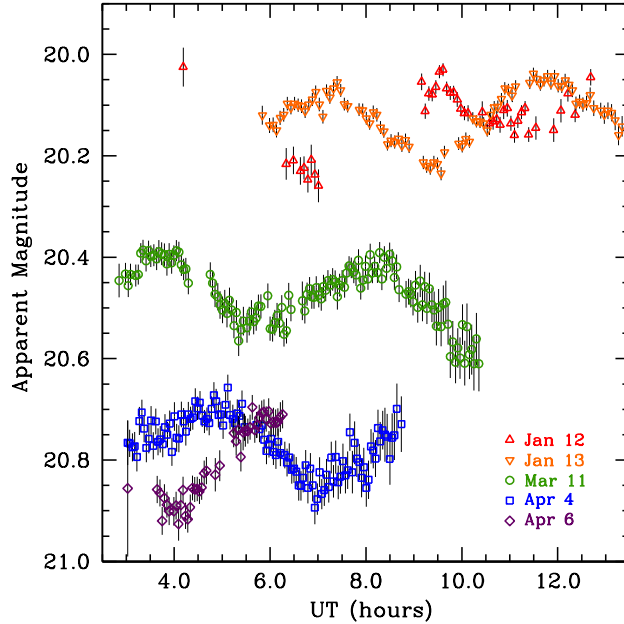


Fig. 1.— Reduced R-band magnitudes (m_R) for our data plotted as a function of UT on each night. The magnitudes have had absolute calibrations, extinction corrections, and comparison star corrections applied and are given in Table 2. The symbols are defined in the legend. Note that while r_H remained approximately constant during the observations, Δ and θ increased, causing the brightness to steadily decrease from month to month.

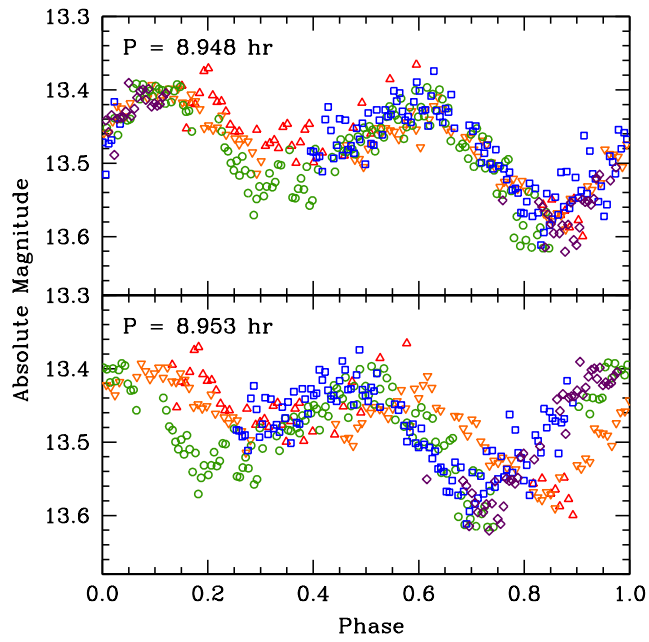


Fig. 2.— The lightcurve data phased to 8.948 hr (top) and 8.953 hr (bottom). Symbols are as given in Figure 1 and the magnitudes are normalized to (1,1,0) as described in the text. The 8.948 hr period is the synodic period expected in 2013 based on the 2010 prograde sidereal solution found in Knight et al. (2012) while the 8.953 hr period is the synodic period expected in 2013 based on the 2010 retrograde sidereal solution. The 8.953 hr period is clearly incompatible with the 2013 data, thus definitively ruling out retrograde rotation.